Talanta 82 (2010) 1826–1838

Contents lists available at ScienceDirect

Talanta

journal homepage: www.elsevier.com/locate/talanta

Monitoring of metabolic profiling and water status of Hayward kiwifruits by nuclear magnetic resonance☆

D. Capitani[a], L. Mannina[b,a,*], N. Proietti[a], A.P. Sobolev[a], A. Tomassini[c], A. Micheli[c], M.E. Di Cocco[c], G. Capuani[c], R. De Salvador[d], M. Delfini[c]

[a] Istituto di Metodologie Chimiche, Laboratorio di Risonanza Magnetica "Annalaura Segre", CNR, I-00015 Monterotondo, Rome, Italy
[b] Dipartimento di Chimica e Tecnologie del Farmaco, Sapienza Università di Roma, Piazzale Aldo Moro 5, I-00185 Rome, Italy
[c] Dipartimento di Chimica, Sapienza Università di Roma, Piazzale Aldo Moro 5, I-00185 Rome, Italy
[d] CRA Centro di Ricerca per la Frutticoltura, Via Fioranello 5, I-00134 Rome, Italy

ARTICLE INFO

Article history:
Received 30 April 2010
Received in revised form 28 July 2010
Accepted 30 July 2010
Available online 7 August 2010

Keywords:
Kiwifruit
NMR
Metabolic profiling
Water status

ABSTRACT

The metabolic profiling of kiwifruit (*Actinidia deliciosa*, *Hayward* cultivar) aqueous extracts and the water status of entire kiwifruits were monitored over the season (June–December) using nuclear magnetic resonance (NMR) methodologies. The metabolic profiling of aqueous kiwifruit extracts was investigated by means of high field NMR spectroscopy. A large number of water-soluble metabolites were assigned by means of 1D and 2D NMR experiments. The change in the metabolic profiles monitored over the season allowed the kiwifruit development to be investigated. Specific temporal trends of aminoacids, sugars, organic acids and other metabolites were observed.

The water status of kiwifruits was monitored directly on the intact fruit measuring the T_2 spin–spin relaxation time by means of a portable unilateral NMR instrument, fully non-invasive. Again, clear trends of the relaxation time were observed during the monitoring period.

The results show that the monitoring of the metabolic profiling and the monitoring of the water status are two complementary means suitable to have a complete view of the investigated fruit.

1. Introduction

The increasing ability of high field NMR spectroscopy to solve spectra of complex mixtures and to recognize and quantify each component without chemical separation, has found a constantly increasing application in metabolomics and food chemistry [1]. ^{1}H high field NMR spectroscopy has shown to be a valuable tool for the qualitative and quantitative analysis of the metabolic profiling of food stuff such as truffles [2], sea bass [3] olive oils [4], tomatoes [5], lettuce [6] and mangoes [7]. The quantitative analysis of the metabolic profiling along with the application of a suitable statistical analysis has allowed food characterization in terms of geographical origin [8], genetic origin [9–14] and farming [3]. The potential of NMR spectroscopy to detect food adulterations has been also demonstrated [15].

In recent years kiwifruit has become an important horticultural crop. For the consumer, desirable attributes of kiwifruit are flavour, fragrance and healthful properties which are obviously due to the fruit chemical composition. In particular, the flavour of the fruit flesh is highly dependent on the balance between soluble sugars and non-volatile organic acids. Besides, different sugars are responsible of different sweetness levels whereas organic acids give a different perception of the acidity. Consequently, qualitative and quantitative analyses of metabolites in kiwifruits are very

Abbreviations: AA, ascorbic acid; ATP, adenosine tri-phosphate; ALA, alanine; ARG, arginine; ASN, asparagine; ASP, aspartate; CHN, choline; CA, citric acid; COSY, correlated spectroscopy; CPMG, Carr Purcell Meiboom Gill; DOSY, diffusion ordered spectroscopy; αFRUfu, α-D-fructofuranose; βFRUfu, β-D-fructofuranose; βFRUpy, β-D-fructopyranose; FRU6P, fructose-6-phosphate; αGAL, α-galactose; βGAL, β-galactose; GAL-U, galactose-U; GARP, globally optimized alternating phase rectangular pulse; GLUtCA, O^3-β-D-glucopyranosyl-*trans*-caffeic acid; GLUcCA, O^3-β-D-glucopyranosyl-*cis*-caffeic acid; αGLC, α-glucose; βGLC, β-glucose; αGLC6P, α-glucose-6-phosphate; βGLC6P, β-glucose-6-phosphate; GLU, glutamate; GLN, glutamine; HMBC, heteronuclear multiple-bond correlation; HSQC, heteronuclear single quantum coherence; ILE, isoleucine; LA, lactic acid; LEU, leucine; LYS, lysine; MA, malic acid; αMAN, α-mannose; βMAN, β-mannose; MI, *myo*-inositol; NOESY, nuclear overhauser and exchange spectroscopy; PGSE, pulsed field gradient spin echo; QA, quinic acid; RAF, raffinose; RIB, ribose; SHA, shikimic acid; SUCR, sucrose; THR, threonine; TOCSY, total correlation spectroscopy; TRP, triptophane; TSP, trimethylsilylpropionate; URI, uridine; VAL, valine; αXYL, α-xylose; βXYL, β-xylose.

☆ In memory of Annalaura Segre, our beloved teacher and friend.

* Corresponding author at: Dipartimento di Chimica e Tecnologie del Farmaco, Sapienza Università di Roma, Piazzale Aldo Moro 5, I-00185 Rome, Italy.
Tel.: +39 06 90672700; fax: +39 06 90672477.
E-mail addresses: luisa.mannina@uniroma1.it, luisa.mannina@imc.cnr.it (L. Mannina).

0039-9140/$ – see front matter © 2010 Elsevier B.V. All rights reserved.
doi:10.1016/j.talanta.2010.07.080

important for the commercial success. The knowledge of nutritional profile of kiwifruits is also extremely important for the industries which extract specific compounds from the fruit to obtain additives for other foodstuffs.

In this framework the knowledge of the metabolic profiling of kiwifruits at different development stages may have an important role in the determination of the most suitable time of harvesting as well as in the quantitative determination of nutrients at different growth times. Various results have been previously reported on the kiwifruit chemical composition using different techniques [16,17]. In particular, HPLC technique has allowed the determination, in kiwi juice, of some classes of compounds such as organic acids, sugars and amino acids [18–20]. ^{1}H NMR spectroscopy has been previously applied for the quantitative analysis of malic and citric acids in kiwifruit juice samples at adjusted pH values [21]. However, at our knowledge, a full high field NMR study for the determination of the metabolic profiling of kiwifruit has not been reported in the literature.

In the present paper, we report an NMR investigation of kiwifruit (*Hayward* cultivar) aqueous extracts. As a non-specific high-throughput analytical method, NMR spectroscopy is well suited to the requirements of metabolic profiling having the advantage to detect signals due to many different classes of compounds in the same experiment. The metabolic profiling of aqueous extracts monitored over a seven months period was determined to investigate the kiwifruit composition at different harvesting times.

Along with a detailed high field NMR study, a low field non-invasive ^{1}H NMR investigation of kiwifruits is also reported. As well known, low field ^{1}H NMR relaxometry is an important tool to investigate the water status in foodstuffs [22]. In fact this methodology allows to obtain information on water compartments, diffusion, and movement, detecting protons predominantly contributed by ^1H_2O contained in foodstuffs. In literature, different foodstuffs, such as mozzarella cheese [23], banana fruits [24], and meat [25] have been investigated by means of low field NMR and important information on the food texture and on the ripening status has been obtained.

It has been shown that the novel recently available low field portable NMR instruments [26,27] provide information on the entire object *in situ* and even if the magnetic field penetrating the object is rather inhomogeneous, useful information can be obtained in many fields of application such as soft matter, plant leaves [28], biological tissues and porous materials [29,30]. Here, we report the water status of the entire kiwifruits monitored over the season by means of a portable unilateral NMR instrument.

2. Materials and methods

2.1. Materials

Hayward kiwifruits were hand harvested in an experimental field located in Lazio region, Italy, over a period beginning in June 2008 and ending in December 2008 carrying out seven campaigns of measurement to monitor a wide range of developing. It is important to point out that the same kiwifruits were used to perform both low field NMR measurements with portable instrument immediately after the harvesting and high field NMR measurements on the aqueous extracts.

2.2. High-resolution NMR measurements

2.2.1. Samples preparation

Fresh cut pulp (1 g) was frozen in liquid N_2, finely powdered, and submitted to an extraction according to the modified [31] Bligh–Dyer methodology [32] with methanol/chloroform/water in 2:2:1 volumetric ratio. Sample was kept at 4 °C for 1 h and then centrifuged for 20 min at 11,000 × *g* (times gravity) at 4 °C. The upper hydroalcolic phase and the lower organic phase were carefully separated and dried under an N_2 flow. The dried phases were stored at −80 °C until the NMR analysis.

2.2.2. NMR spectra

The dry residue of the hydroalcolic phase was dissolved in a D_2O phosphate buffer (100 mM, pH 7.2) containing 3-(trimethylsilyl)-propionic-2,2,3,3,-d_4 acid sodium salt (TSP, 2 mM) as internal standard.

The NMR spectra of kiwifruit aqueous extracts were recorded at 27 °C on a Bruker AVANCE AQS600 spectrometer operating at the proton frequency of 600.13 MHz and equipped with a Bruker multinuclear *z*-gradient inverse probehead. ^{1}H spectra were referenced to TSP signal (δ = 0.00 ppm) whereas ^{13}C spectra were referenced to the CH-1 resonance of α-D-glucose (δ = 93.10 ppm).

The ^{1}H spectra of the aqueous extracts were acquired by co-adding 512 transients with a recycle delay of 3 s and using a 90° pulse of 10.8 μs, 32K data points. The water signal was suppressed using a solvent presaturation (NOESY-presaturation scheme) during the relaxation delay and a mixing time of 160 ms [33]. In order to minimize the variability of the signals intensity due to water suppression, a careful calibration of the soft pulse for water suppression was always performed.

2D NMR experiments, namely ^{1}H–^{1}H COSY, ^{1}H–^{1}H TOCSY, ^{1}H–^{1}H NOESY, ^{1}H–^{13}C HSQC and ^{1}H–^{13}C HMBC [33], were performed using the same experimental conditions previously reported [2]. The mixing time for the ^{1}H–^{1}H TOCSY was 80 ms, the mixing time for ^{1}H–^{1}H NOESY was 400 ms. The HSQC experiments were performed using a coupling constant $^1J_{C-H}$ of 150 Hz and the ^{1}H–^{13}C HMBC experiments were performed using a delay for the evolution of long-range couplings of 80 ms.

The {^{1}H}-decoupled ^{31}P NMR experiments were performed at 242.94 MHz by co-adding 1500 transients with a recycle delay of 7 s, a 20 kHz spectral width, 8K data points, a GARP pulse sequence for proton decoupling, and a 90° ^{31}P pulse of 14 μs. Chemical shifts for the ^{31}P spectrum were given in ppm with respect to an external standard of 85% H_3PO_4.

The ^{1}H–^{31}P HMBC spectra were obtained using a recycle delay of 2 s, a 90° ^{1}H pulse of 11 μs and a 90° ^{31}P pulse of 14 μs and 6 and 10 kHz spectral widths in proton (F2) and phosphorus (F1) dimensions respectively, 1K data points in F2, 512 increments in F1, and a linear prediction up to 1K points in F1. Data were processed using un-shifted sinusoidal window functions in both dimensions. The delay for the evolution of long-range couplings was 80 ms.

Pulsed field gradient spin echo (PGSE) experiments [34,35] were performed with a pulsed field gradient unit producing a magnetic field gradient in the *z*-direction with a strength of 55.4 G cm^{-1}. The stimulated echo pulse sequence using bipolar gradients with a longitudinal eddy current delay was used. The strength of the sine-shaped gradient pulse with a duration of 1.4 ms, was logarithmically incremented in 32 steps, from 2% up to 95% of the maximum gradient strength, with a diffusion time of 120 ms and a longitudinal eddy current delay of 25 ms. After Fourier transformation and a baseline correction, the diffusion dimension was processed using the DOSY [36,37] subroutine of the Bruker TOPSPIN 1.3 software package.

The detection limit of a given metabolite, analyzed in a 5 mm tube using 1D ^{1}H NMR spectroscopy at high field (11–16 T) is about 50 μM.

2.2.3. Statistical analysis

In order to perform a comparison between ^{1}H spectra of different kiwifruits, the signal linewidth of each specific resonance has to be the same in all analyzed spectra. It can be obtained by using

always the same experimental protocol such as sample preparation, acquisition, and processing procedures. In these conditions, the intensity (height of the resonance) as well as the integral is proportional to the molar concentration. Since the measurement of the intensity is much less affected by peaks overlapping with respect to the integral measurement, in the present work the peak intensity was used for the statistical analysis.

The intensity of selected ^{1}H resonances due to water-soluble metabolites was measured with respect to the intensity of TSP signal normalized to 1000 and used as internal standard. The measured resonances, see list of abbreviation and Table 1, are due to U1 (0.88 ppm), LEU (0.96 ppm); ILE (1.03 ppm); VAL (0.99 ppm); U2 (1.29 ppm); THR (1.33 ppm); LA (1.37 ppm); U3 (1.46 ppm); ALA (1.49 ppm); ARG (1.66 ppm); QA (4.17 ppm); GLN (2.48 ppm); GLU (2.52 ppm); MA (4.39 ppm); CA (2.73 ppm); ASN (2.97 ppm); CHN (3.20 ppm); MI (3.30); βFRUpy (3.58 ppm); βGAL (4.60 ppm); βGLC (4.67 ppm); AA (4.75 ppm); GLUtCA (6.41 ppm); GAL-U (5.16); αGLC (5.25 ppm); SUCR (5.42 ppm); U5 (5.51 ppm); U6 (5.69 ppm); GLUcCA (5.96 ppm); U7 (5.89 ppm); U10 (6.13 ppm); U11 (6.49 ppm); U12 (6.60 ppm); SHA (6.68 ppm); U14 (7.08 ppm); U15 (7.10 ppm); U16 (7.11 ppm); U17 (7.41); TRP (7.55); URI (7.98 ppm).

The statistical processing of the NMR data was performed using the Unscrambler 9.8 software (CAMO Software, Oslo, Norway).

In order to evaluate the reproducibility of NMR measurements three portions of aqueous extract from the same fruit were used. The samples were prepared and analyzed according to method reported above, and the intensity of selected signals was measured. The obtained values showed a very good repeatability (standard deviation <2.5%) for all signals.

The intensities of each selected NMR signal were reported as elements of a data matrix, where each sample is represented by a row and each NMR signal is represented by a column. The harvesting months, from June to December, were added as a new column: this is the variable, often referred as the "external" variable, against which the multivariate regression was performed. The matrix was pre-processed by mean centring and scaling: the means of each column were set to zero whereas their standard deviations were set to one [38]. This widely used procedure, applied to the data matrix prior to partial least squares (PLS) analysis, allows to compare the co-variations of the signals independently on their numerical size, keeping intact the factorial structure.

Four samples out of 55 were detected as outliers and discarded from the analysis. PLS was performed on the remaining dataset and the model was validated through a full cross-validation test procedure. The significance of the correlation between the original variables and the PLS models was assessed by the uncertainty test [39,40].

2.3. ^{1}H low field measurements using portable unilateral NMR

All measurements were performed using a portable unilateral NMR instrument from Bruker Biospin. The probe head of the instrument is made of a U shaped magnet assembled with two permanent magnets mounted on an iron yoke and including a radio-frequency resonator [41,42].

The campaign of measurements was carried out from June 2008 to December 2008. The measurements were carried out non-destructively on kiwifruits detached from the plants. The sampled kiwifruit was positioned in contact with the probehead. Measurements were performed on the entire fruit using a probehead operating at 16 MHz and allowing the measurements within a slice of the fruit at a depth of about 0.5 cm from the surface.

The 90° pulse was 10.4 μs and the dead time was 15 μs. Since in a non-homogenous magnetic field the NMR signal decays very quickly, the NMR signal must be recovered stroboscopically [29]. Therefore the signal intensity or integral is actually the intensity or integral of the signal resulting after applying the Hahn echo pulse sequence [43].

Transverse T_2 relaxation times were measured with a CPMG pulse sequence [44,45], 2048 echoes were collected using an echo time of 150 μs. The echo time of 150 μs allowed the detection of long T_2 relaxation times occurring at an advanced stage of ripening disregarding the signal due to the water strictly associated with cell walls. A recycle time of 3 s was used and 512 scans were collected. The same experimental conditions were always used over the campaign of measurements.

Experimental data obtained with the CPMG pulse sequence were fit to a bi-exponential function. From the best fit procedure two T_2 components were obtained, namely T_{2a} and T_{2b}. In order to better visualize the experimental data, a regularized inverse Laplace transformation [46] was applied to the CPMG decays. Using this transformation data were represented as a distribution of T_2 relaxation times.

3. Result and discussion

In order to have a complete view of the kiwifruit a detailed study of the metabolic profiling of the aqueous extracts was performed. The nutritional composition of kiwifruits as well as their shelf life depend strongly on the harvesting time. A fruit harvested too early has a low level of carbohydrates whereas a fruit harvested too late may have a reduced shelf life being soften and subjected to mold. Many kiwifruits are harvested when they are mature but not fully ripe having the major amount of carbohydrates present in the starch form. The progressive disappearance of starch is accompanied by a consistent increase in the concentration of soluble sugars [47].

The growth of kiwifruits over the season was investigated using two different complementary NMR methodologies: a high field NMR study of kiwifruit aqueous extracts, to monitor changes in the metabolic profiling and a low field NMR investigation directly on entire kiwifruits to monitor, non-destructively, the water status at different stages of growth.

3.1. NMR metabolic profiling of aqueous kiwifruit extracts: implications in kiwifruit development

The assignment of the ^{1}H spectrum of kiwifruit aqueous extract, see Fig. 1, obtained by 1D and 2D NMR experiments and literature data [1] and, when necessary, by adding standard compounds, is reported in Table 1 and will be discussed for class of compounds.

The analysis of the metabolic profiling of the extracts over a seven months period showed some interesting trends which will be discussed for class of compounds.

3.1.1. Organic acids

The quantitative HPLC determination of organic acids, namely malic acid (MA), citric acid (CA), quinic acid (QA), ascorbic acid (AA), tartaric and isocitric acids in trace, in kiwi juices and puree has been previously reported [18,20,21]. In the ^{1}H spectrum of kiwifruit extracts MA, CA, QA, AA were identified by means of their diagnostic peaks. Besides, lactic acid (LA) was also identified for the first time in the kiwifruit extract as well as shikimic acid (SHA) although it is present only at the very first stages of growth. The assignment of shikimic acid was obtained by means of the characteristic spin system in the TOCSY map, see Fig. 2A.

Shikimic acid (SHA) is detectable only in June and July whereas it is not more detectable at a later stage of development, see Fig. 3. At our knowledge, the presence of shikimic acid has not been previously reported in kiwifruit probably because this acid appears

Table 1
Summary of the metabolites identified in the 600 MHz ^{1}H spectrum of the aqueous extract of kiwifruits.

Compound	Assignment	^{1}H (ppm)	Multiplicity: *J* (Hz)	^{13}C (ppm)
Organic acids				
Malic acid (MA)	α-CH	4.39*		69.95
	CH_2 β,β′	2.81, 2.64		41.54
	–CH	2.64		41.54
	–COOH			178.18
	–COOH			180.69
Citric acid (CA)	α,γ-CH	2.73*	d: 15.8	45.20
	α′,γ′-CH	2.84		45.20
	β-C			75.41
	1,5-COOH			177.11
	6-COOH			180.79
Quinic acid (QA)	CH_2-1,1′	1.89, 2.10		41.72
	CH-2	4.03		67.97
	CH-3	3.56		76.32
	CH-4	4.17*		71.44
	CH_2-5,5′	2.00, 2.06		38.30
	C-6			77.94
	COOH			181.97
Ascorbic acid (AA)	CH_2-2′	3.76		63.50
	CH-1′	4.06		64.45
	CH-5	4.75*		78.32
	C-4			167.23
	C-3			116.37
	C-2			176.71
Lactic acid (LA)	α-CH	4.21		
	CH_3	1.37*	d: 7.0	20.9
Shikimic acid (SHA)	CH_2-7	2.24, 2.77		32.63
	CH-6	4.03		
	CH-5	3.77		67.80
	CH-4	4.45	t: 4.3	67.16
	CH-3	6.68**		134.80
Carbohydrates				
α-Glucose (αGLC)	CH-1	5.25*		93.10
	CH-2	3.55		72.4
	CH-3	3.72		73.77
	CH-4	3.42		70.696
	CH-5	3.84		72.49
	CH_2-6,6′	3.72, 3.90		61.78
β-Glucose (βGLC)	CH-1	4.67*		96.91
	CH-2	3.26		75.2
	CH-3	3.50		76.85
	CH-4	3.42		70.70
	CH-5			
	CH_2-6,6′	3.74, 3.91		61.78
Sucrose (SUCR)	GLC CH-1	5.42*		93.24
	CH-2	3.59		72.15
	CH-3	3.79		73.63
	CH-4	3.48		70.27
	CH-5	3.85		73.46
	CH_2-6	3.82		61.19
	FRU CH_2-1′	3.69		62.36
	C2′			104.77
	CH-3′	4.22		77.45
	CH-4′	4.06		75.09
	CH-5′	3.90		82.39
	CH_2-6	3.82		63.42
Myo-inositol (MI)	CH-1	4.08		73.2
	CH-2,5	3.55		
	CH-3,6	3.63		73.47
	CH-4	3.30*		75.39
α-Galactose (αGAL)	CH-1	5.30		93.44
	CH-2	3.81		
	CH-3	3.87		
	CH-4	3.95		
	CH-5	4.00		
	CH-6	3.76		
β-Galactose (βGAL)	CH-1	4.60***	d: 8.0	
	CH-2	3.51		
	CH-3	3.65		
	CH-4	3.94		
α-D-Fructofuranose (αFRUfu)	C-2			102.4
	CH-3	4.13		83.0
	CH-5	4.04		82.41
β-D-Fructofuranose (βFRUfu)	CH_2-1,1′			
	CH-2			105.53
	CH-3	4.12		76.54

Table 1 (*Continued*)

Compound	Assignment	^{1}H (ppm)	Multiplicity: *J* (Hz)	^{13}C (ppm)
	CH-4	4.12		75.53
	CH-5	3.83		81.67
	CH_2-6,6′	3.68, 3.82		63.37
β-D-Fructopyranose (βFRUpy)	CH_2-1,1′	3.72, 3.58*		64.97
	CH-3	3.81		68.6
	CH-4	3.91		70.71
	CH-5	4.01		70.27
α-Xylose (αXYL)	CH-1	5.21	d: 3.7	94.16
	CH-2	3.53		
	CH-3	3.67		
β-Xylose (βXYL)		4.56	d: 7.9	
Raffinose (RAF)	GLC CH-1	5.45	d: 3.9	
	CH-2	3.59		
	CH-3	3.79		
	CH-4	3.48		
	GAL CH-1	5.01	d: 3.7	
	CH-2	3.86		
	CH-3	3.91		
	CH-4	4.02		
α-Mannose (αMAN)	CH-1	5.19	d: 1.7	
β-Mannose (βMAN)	CH-1	4.91	d: 1.0	
Galactose-U (GAL-U)	GAL CH-1	5.16*	d: 4.0	96.40
	CH-2	3.88	d: 4, 10.2	69.33
	CH-3	3.97	d: 10.2, 3.8, 1.3	70.35
	CH-4	4.03	d: 3.8, 1.3	
	U	4.27	t: 2.6	69.20
	U	3.63	dd: 9.5, 2.2	
	U	3.52	dd: 9.5, 2.2	
	U	3.33	t: 9.4	
	U	3.67	dd: 9.0, 10.0	
	U	3.76	dd: 9.0, 10.0	
Fructose-6P (FRU6P)	CH_2-6,6′	3.85, 3.95		(^{31}P) 1.15
α-Glucose-6P (αGLC6P)	CH_2-6,6′	4.12, 4.16		(^{31}P) 1.42
β-Glucose-6P (βGLC6P)	CH_2-6,6′	4.05, 4.08		(^{31}P) 1.42
Rhamnose residue (oligosaccharide)	CH_3	1.31, 1.30 (α e β forms)	d: 6.5; d: 6.2	
	CH	3.45, 3.49, 3.90		
Amino acids				
Alanine (ALA)	α-CH	3.81		51.53
	β-CH_3	1.49*	d: 7.3	17.25
	COOH			176.91
	γ-CH_2	3.04		40.04
Glutamine (GLN)	α-CH	3.80		55.32
	–CH_2 β,β′	2.16, 2.12		27.21
	γ-CH	2.48*		32.62
	$CO(NH_2)$			180.12
	COOH			175.47
Threonine (THR)	α-CH	3.62		–
	β-CH	4.28		66.25
	γ-CH_3	1.33*		20.46
Arginine (ARG)	α-CH	3.79		
	β-CH_2	1.66*, 1.72		25.0
	γ-CH_2	1.91		28.53
	δ-CH_2	3.26		41.54
Glutamate (GLU)	α-CH	3.82		55.61
	CH_2 β,β′	2.17		
	γ-CH	2.52*		
Asparagine (ASN)	α-CH	4.02		52.38
	β,β′ CH_2	2.88, 2.97*		35.55
	γ-COOH			174.4
	COOH			174.4
Aspartate (ASP)	α-CH	3.91		53.25
	β,β′ CH_2	2.81, 2.71		37.60
Valine (VAL)	α-CH	3.62		
	β-CH	2.28		
	γ-CH_3	0.99*	d: 7.0	
	γ′-CH_3	1.05		
Leucine (LEU)	α-CH	3.66		
	β-CH_2	1.73		
	γ-CH	1.69		
	δ-CH_3, δ′-CH_3	0.96*		
Isoleucine (ILE)	δ-CH_3	0.95	t: 7.0	
	γ-CH_3	1.03*	d: 6.8	
Lysine (LYS)	α-CH	3.79		
	β-CH_2	1.92		
	γ-CH_2	1.46		
	δ-CH_2	1.73		
	ε-CH_2	3.04	t: 7.7	

Table 1 (*Continued*)

Compound	Assignment	^{1}H (ppm)	Multiplicity: *J* (Hz)	^{13}C (ppm)
Triptophane (TRP)	CH-4	7.70	d: 8.0	119.32
	CH-7	7.55*	d: 8.0	113.05
	CH-6	7.29		123.12
	CH-5	7.19	t: 7.0	120.43
	α-CH	3.99		55.16
	β-CH	3.00		39.74
	β′-CH	3.32		39.74
	δ-CH_3, δ′-CH_3			
γ-Aminobutyrate (GAB)	α-CH_2	2.43		
	β-CH_2	1.94		23.27
	γ-CH_2	3.04		40.04
Miscellaneous metabolites				
Choline (CHN)	$N(CH_3)_3^+$	3.20	s	54.9
Adenosine tri-phosphate (ATP)	CH-2	8.58	s	
	CH-8	8.36	s	
	RIB C1′H	6.19	d: 5.7	88.41
	RIB C2′H	4.81		
	RIB C3′H	4.58		
	RIB C4′H	4.52		
	RIB C5′H	–		
O^3-β-D-Glucopyranosyl-*trans*-caffeic acid (GLUtCA)	C1			128.30
	CH-2	7.48	d: 2.2	116.82
	C3			148.94
	C4			159.58
	CH-5	7.04	d: 8.3	117.72
	CH-6	7.33	dd: 8.3, 2.2	125.98
	CH-7	7.66	d: 16	145.67
	CH-8	6.41*	d: 16	116.88
	COOH			173.29
	CH-1′	5.17	d: 7.7	102.06
	CH-2′	3.67		
	CH-3′	3.67		
	CH-4′	3.55		
	CH-5′	3.76		
	CH-6′	3.97		
O^3-β-D-Glucopyranosyl-*cis*-caffeic acid (GLUcCA)	C1			
	CH-2	7.49	d: 2	117.85
	C3			
	C4			
	CH-5	6.98	d: 8.3	117.90
	CH-6	7.16	dd: 8.3, 2.0	126.71
	CH-7	6.85	d: 12.5	
	CH-8	5.96**	d: 12.5	119.32
	COOH			
	CH-1′	5.04	d: 7.7	102.20
	CH-2′	3.63		
	CH-3′	3.63		
	CH-4′	3.57		
	CH-5′	3.71		
	CH-6′	3.96		
Uridine (URI)	CH-5 ring	5.97	d: 8.0	103.73
	CH-6 ring	7.98*	d: 8.0	
	RIB CH-1	5.98	d: 4.2	89.53
	CH-2	4.38		73.45
	CH-3	4.30		
	CH-5			
Unassigned signals				
U1		0.88**		
U2		1.29***		
U3		1.46		
U5		5.51*		
U6		5.69*		
U7		5.89*		
U10		6.13**		
U11		6.49*		
U12		6.60**		
U14		7.08***		
U15		7.10**		
U16		7.11*		
U17		7.41**		
U18		8.61		

Abbreviations are reported. Signals selected for the statistical analysis are denoted by one asterisk if present over the season, by two asterisks if present only in the first part of the season and by three asterisks if present only in the last part of the season.

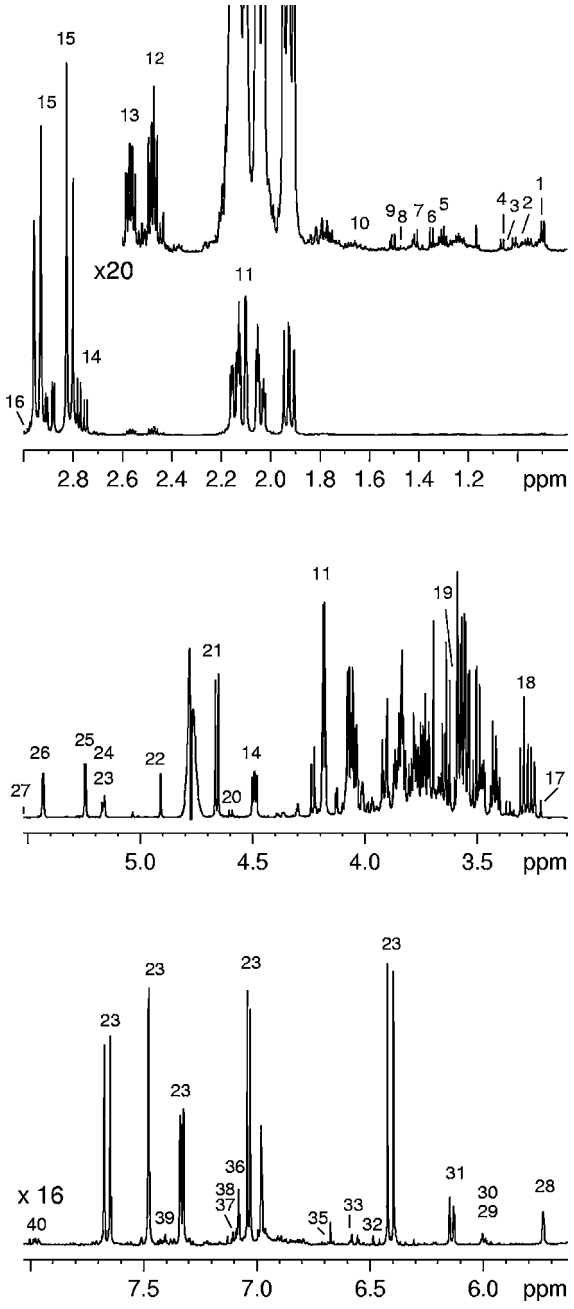

Fig. 1. 600.13 MHz ^{1}H NMR spectrum of a kiwifruit extract in aqueous solution at 27 °C. The assignment of some peaks is reported: **1**, U1 (0.88); **2**, LEU (0.96); **3**, ILE (1.03); **4**, VAL (0.99); **5**, U2 (1.29); **6**, THR (1.33); **7**, LA (1.37); **8**, U3 (1.46); **9**, ALA (1.49); **10**, ARG (1.66); **11**, QA (4.17); **12**, GLN (2.48); **13**, GLU (2.52); **14**, MA (4.39); **15**, CA (2.73); **16**, ASN (2.97); **17**, CHN (3.20); **18**, MI (3.30); **19**, FRUpy (3.58); **20**, βGAL (4.57); **21**, βGLC (4.67); **22**, AA (4.75); **23**, GLUtCA (6.41); **24**, GAL-U (5.16); **25**, αGLC (5.25); **26**, SUCR (5.42); **27**, U5 (5.51); **28**, U6 (5.69); **29**, GLUcCA (5.96); **30**, U7 (5.89); **31**, U10 (6.13); **32**, U11 6.49; **33**, U12 (6.60); **35**, SHA (6.68); **36**, U14 (7.08); **37**, U15 (7.10); **38**, U16 (7.11); **39**, **U17** (7.41); **40**, URI (7.98).

only at the early stage of development whereas most metabolomic studies have been focused on the later stage.

Malic acid (MA) and citric acid (CA) reach the highest concentration in August remaining rather constant in the successive period, see CA histogram in Fig. 3. Quinic acid (QA) and ascorbic acid (AA) are already present in June, then their content decreases, see AA and QA histograms in Fig. 3.

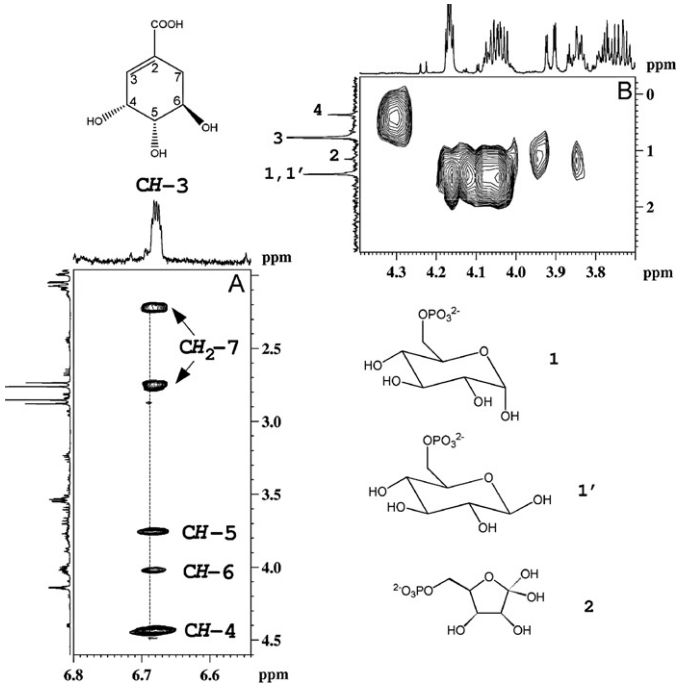

Fig. 2. (A) Expansion of ^{1}H–^{1}H TOCSY map, the spin system of shikimic acid is shown together with its structure. (B) ^{1}H–^{31}P HMBC map of an aqueous extract of kiwifruit. The ^{1}H and the ^{31}P{^{1}H}-decoupled NMR spectra are reported as projections in the F2 and F1 dimensions, respectively. **1**, **1′**, α-Glucose-6-phosphate and β-glucose-6-phosphate; **2**, fructose-6-phosphate; **3**, orthophosphate; **4**, unassigned compound.

3.1.2. Sugars

Different sugars are present in kiwifruits. Glucose (GLC), sucrose (SUCR), fructose (FRU) previously identified by liquid chromatography [20] were found in the ^{1}H spectrum. Galactose (αGAL, βGAL), xylose (αXYL, βXYL), mannose (αMAN, βMAN) and raffinose (RAF) were also identified by means of diagnostic anomeric ^{1}H doublets, see Table 1, by 2D experiments and by adding the corresponding standard compounds. At our knowledge, raffinose was identified for the first time in aqueous kiwifruit extracts. An important diagnostic tool for the identification of raffinose was the DOSY map, data not reported, which clearly shows that the anomeric signals at 5.45 and 5.01 ppm, ascribed to the glucose and galactose units respectively, have a self-diffusion coefficient minor than the sucrose self-diffusion coefficient, in agreement with a trisaccharidic structure. The galactose and glucose units were fully assigned whereas, due to the signals overlapping, it was not possible to assign the fructose unit.

The anomeric doublet at 5.16 ppm is possibly due to a disaccharide having a galactosyl unit. The chemical shifts of the spin system at 5.16, 3.88, 3.97 and 4.03 ppm are in agreement with the chemical shifts of galactosyl units reported in literature for galactoglucomannan in kiwifruit extracts [48]. Moreover, the DOSY map, data not reported, shows that the anomeric signal has a self-diffusion coefficient close to that of sucrose signal, therefore suggesting a disaccharide unit, GAL-U.

The presence of glucose-6P (αGLC6P, βGLC6P), fructose-6P (FRU6P) and orthophosphate was evidenced by {^{1}H}-decoupled ^{31}P NMR spectra. Besides, the long-range contacts observed in the ^{1}H–^{31}P HMBC map allowed the assignment of methylene protons in position 6 of glucose-6P and fructose-6P, see Table 1 and Fig. 2B. It is worth to note that both α and β anomers of glucose-6P were detected. The {^{1}H}-decoupled ^{31}P NMR spectrum is reported as projection in F1 dimension. The assignment was further confirmed by adding the corresponding standard compounds.

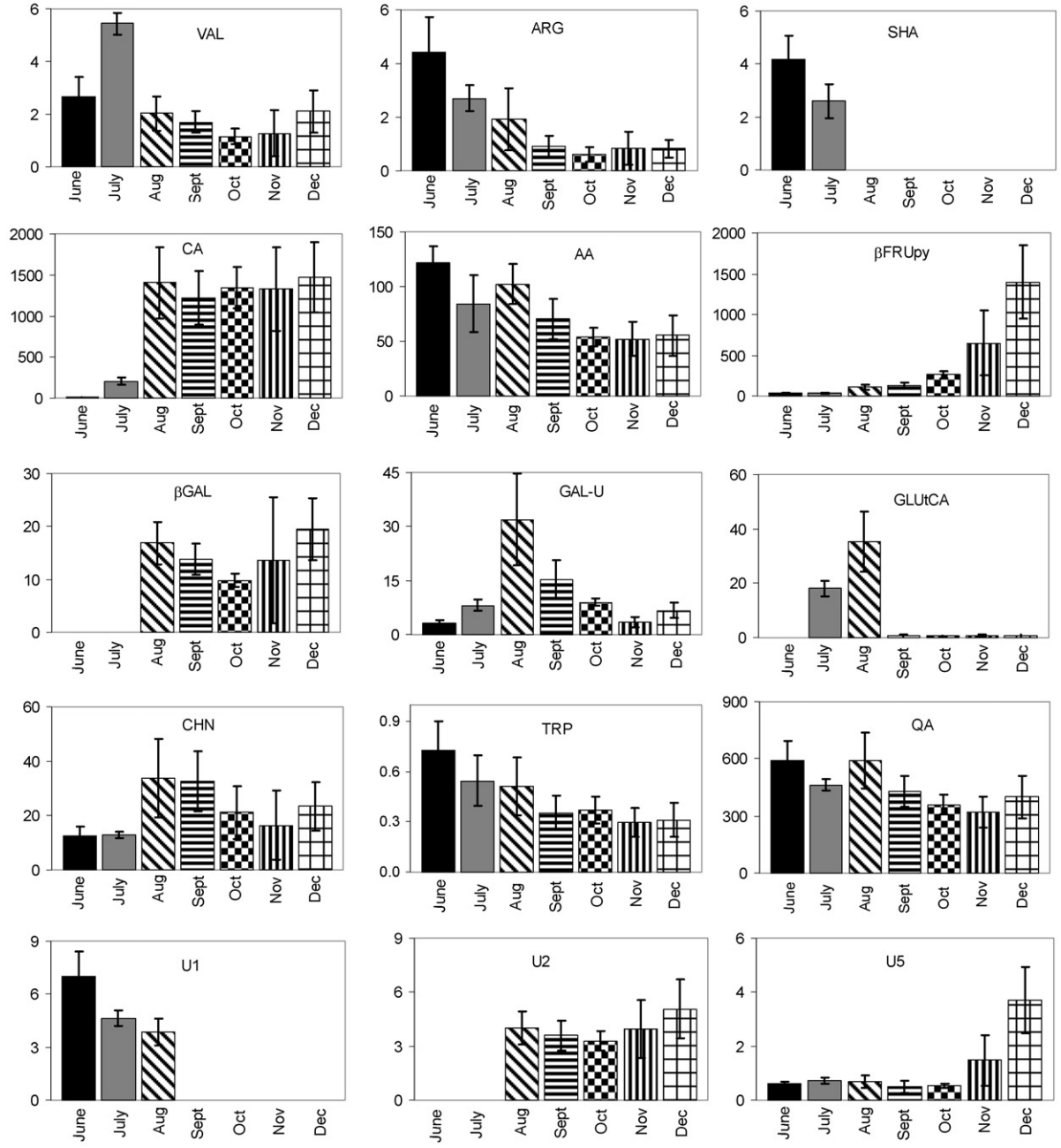

Fig. 3. Histograms resulting from the quantitative NMR spectroscopic analysis of some metabolites present in aqueous extracts of kiwifruits. The relative molecular abundance is reported vs. the harvesting month. Data shown are means ± SE.

A typical spin system of a rhamnose residue was also observed in the TOCSY map. The DOSY map (data not reported), of the rhamnose residue (CH_3 at 1.30 and 1.31 ppm for α and β form respectively, see Table 1) shows a self-diffusion coefficient corresponding to a molecular weight of 0.8–0.9 kDa thus suggesting the oligomeric nature of the compound.

As expected, the content of some sugars such as SUCR, αGLC, βGLC and βFRUpy increases during the growth reaching the highest value in December, see βFRUpy histogram in Fig. 3. Galactose signal starts to be detectable in August, then decreases until October and then increases again, see the histogram in Fig. 3. The GAL-U disaccharide, not yet completely assigned, and *myo*-inositol (MI) show a concentration increase until August followed by a clear decrease, see GAL-U histogram in Fig. 3.

Myo-inositol previously identified in kiwifruit by HPLC [49] was identified in the ^{1}H spectrum by means of the characteristic spin system in the TOCSY map and by adding the corresponding standard compound. *Myo*-inositol was also previously [50] identified in kiwifruit by enzymatic test and by ^{13}C NMR after purification by Ca^{++}-complexation chromatography.

3.1.3. Free amino acids

The ^{1}H spectrum of kiwifruit extracts allowed the free amino acids composition to be obtained. Thirteen amino acids, namely, ALA, GLN, THR, ARG, GLU, ASN, ASP, VAL, LEU, ILE, TRP, LYS and GAB were identified, see Table 1.

Some amino acids such as VAL, LEU, ILE, THR, GLU, and ASN increase during the first harvesting period reaching the highest value in July or in August. After this time a concentration decrease is clearly observable, see as an example the histogram of the average values and the standard errors of VAL reported in Fig. 3. In the case of ALA, ARG, GLN, and TRP the highest concentration is found in

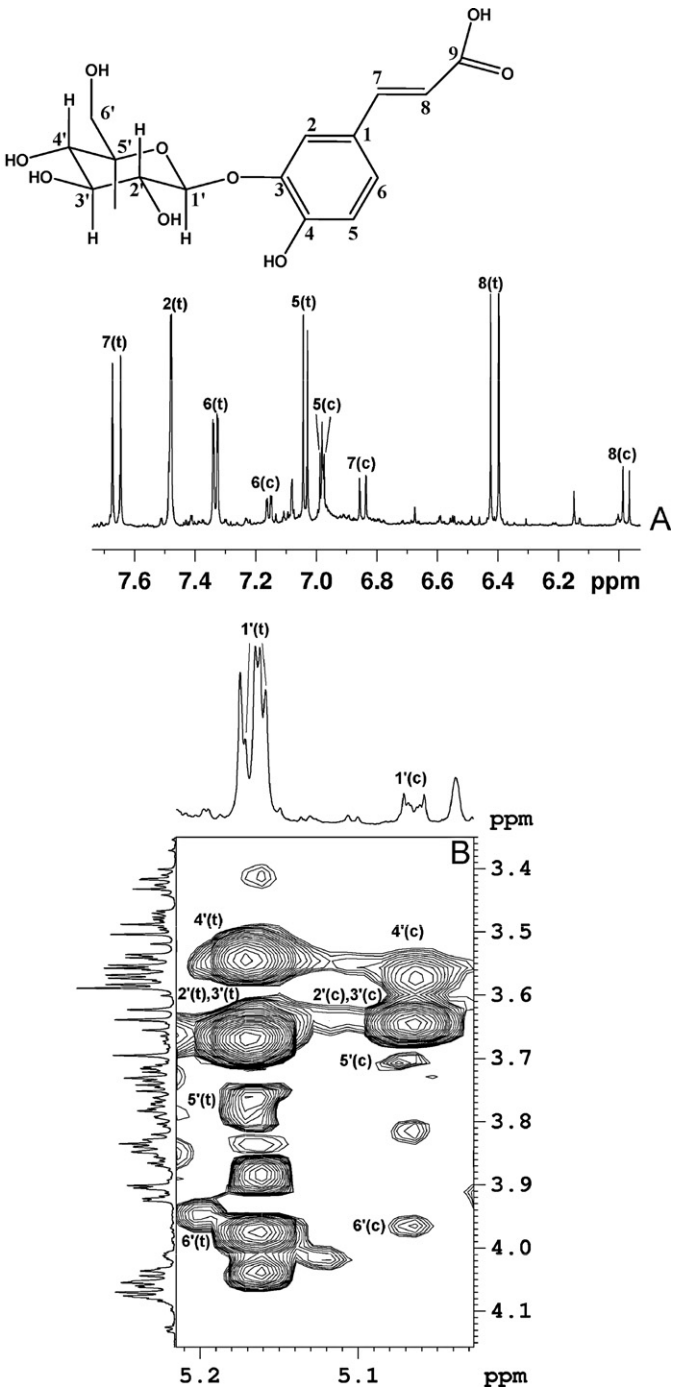

Fig. 4. (A) ^{1}H expanded spectral region and assignment of aromatic and vinyl protons of O^3-β-glucopyranosyl-*trans*-caffeic acid and O^3-β-glucopyranosyl-*cis*-caffeic acid (c = *cis*; t = *trans*). (B) Expansion of ^{1}H–^{1}H TOCSY map, the proton spin system of the glucopyranosyl mojety of O^3-β-glucopyranosyl-caffeic acid is shown.

June, then a decrease is observed, see as an example the histogram of ARG in Fig. 3.

3.1.4. Miscellaneous compounds

Choline was identified by means of diagnostic chemical shift of the methyls signal at 3.20 ppm and adding the corresponding standard compound. The presence of ATP was revealed by adding the corresponding standard compound.

O^3-β-Glucopyranosyl-*trans*-caffeic acid, see the sketch reported in Fig. 4, was also identified for the first time in kiwifruit, along with the *cis* isomer present only in a low amount. Both compounds were previously detected by NMR in poplar xylem [51]. The 5.95–7.70 ppm spectral range of the proton spectrum along with the resonances assignment of the *trans* (t) and *cis* (c) isomers are reported in Fig. 4A. The doublets at 7.66 and 6.41 ppm with a coupling constant of 16 Hz were diagnostic of the presence of the double bound of the *trans* isomer, whereas the doublets at 6.85 and 5.98 ppm with a coupling constant of 12.5 Hz were diagnostic of the presence of the *cis* isomer, see Fig. 4A. Aromatic protons were identified in positions 2 (doublets at 7.48 (*trans*) and 7.49 (*cis*) with a coupling constant of 2 Hz), in position 5 (doublets at 7.04 (*trans*) and 6.98 (*cis*) with a coupling constant of 8.3 Hz), and in position 6 (doublets of doublets at 7.33 (*trans*) and 7.16 (*cis*) with coupling constants of 8.3 and 2.2 Hz). The HMBC experiment was also an important tool allowing the detection of a long-range contact between the vinyl proton in position 8 (6.41 ppm) and the carboxyl carbon 9 at 173.29 ppm. Long-range contacts were found between the aromatic proton in position 2 (7.48 ppm) and the quaternary carbon C4 (159.58 ppm) and between the vinyl proton in position 7 (7.66 ppm) and the quaternary aromatic carbon C1 (128.30 ppm). A long-range contact diagnostic of the derivatization of the aromatic ring in position 3 was found between the anomeric proton 1′ (5.17 ppm) and the aromatic quaternary carbon C3 (148.94 ppm). Besides, in the NOESY map a crosspeak was observed between the anomeric proton 1′ (5.17 ppm) and the aromatic proton in position 2 (7.48 ppm). The TOCSY experiment allowed the identification of the protons of the glucopyranosyl mojety, see Fig. 4B. With the PGSE experiment it was possible to establish that the compound had a self-diffusion coefficient and, therefore, a molecular weight, very similar to that of sucrose. Note that the molecular weight of O^3-β-glucopyranosyl-caffeic acid is 358.24 Da.

GLUtCA, detectable from July, reaches the maximum concentration in August then its concentration is drastically reduced, see the histogram in Fig. 3.

Uridine was identified by means of the diagnostic doublets at 7.98 and 5.97 ppm, due to the uracyl aromatic ring and the doublet of the ribose anomeric proton at 5.98 ppm which showed correlations with CH-2 at 4.38 and CH-3 at 4.30 ppm of ribose in the TOCSY map.

Choline (CHN) and uridine (URI) show a concentration increase until August followed by a decrease, see CHN histogram in Fig. 3.

3.1.5. Unassigned signals

U1, U12, U15 and U17 unassigned signals are present only in the first three to four harvesting months, see U1 histogram in Fig. 3, whereas U2 and U14 begin to be detectable only in August, see U2 histograms in Fig. 3, then U2 remains rather constant whereas U14 is drastically reduced. U5 and U7 signals increase in November and December, see U5 histogram in Fig. 3, whereas U6 and U11 reach the maximum concentration in the early harvesting months, then a slight decrease occurs.

This analysis clearly shows that some metabolites are always present although in different concentration, whereas other metabolites are present only in some months.

To analyze the multivariate structure of the data the PLS analysis was applied to the intensity of 29 ^{1}H resonances always present during the investigated period. Fig. 5A shows a PLS plot of samples scores (PC1 vs. PC2). These first two PCs account for the 95% of the variability within the data, PC1 providing for the 91% and PC2 for the 4%. A clear grouping of the samples according to the harvesting month is observable. Samples collected in June, July and August are well grouped according to the specific campaign of measurement and separated mainly along PC2. The other samples collected later in the season appear separated according to the specific campaign mainly along PC1. It is important to notice that the effect of the growth is visible as a trend along PC1. In fact, the centroid of each campaign group moves toward high PC1 values according to the

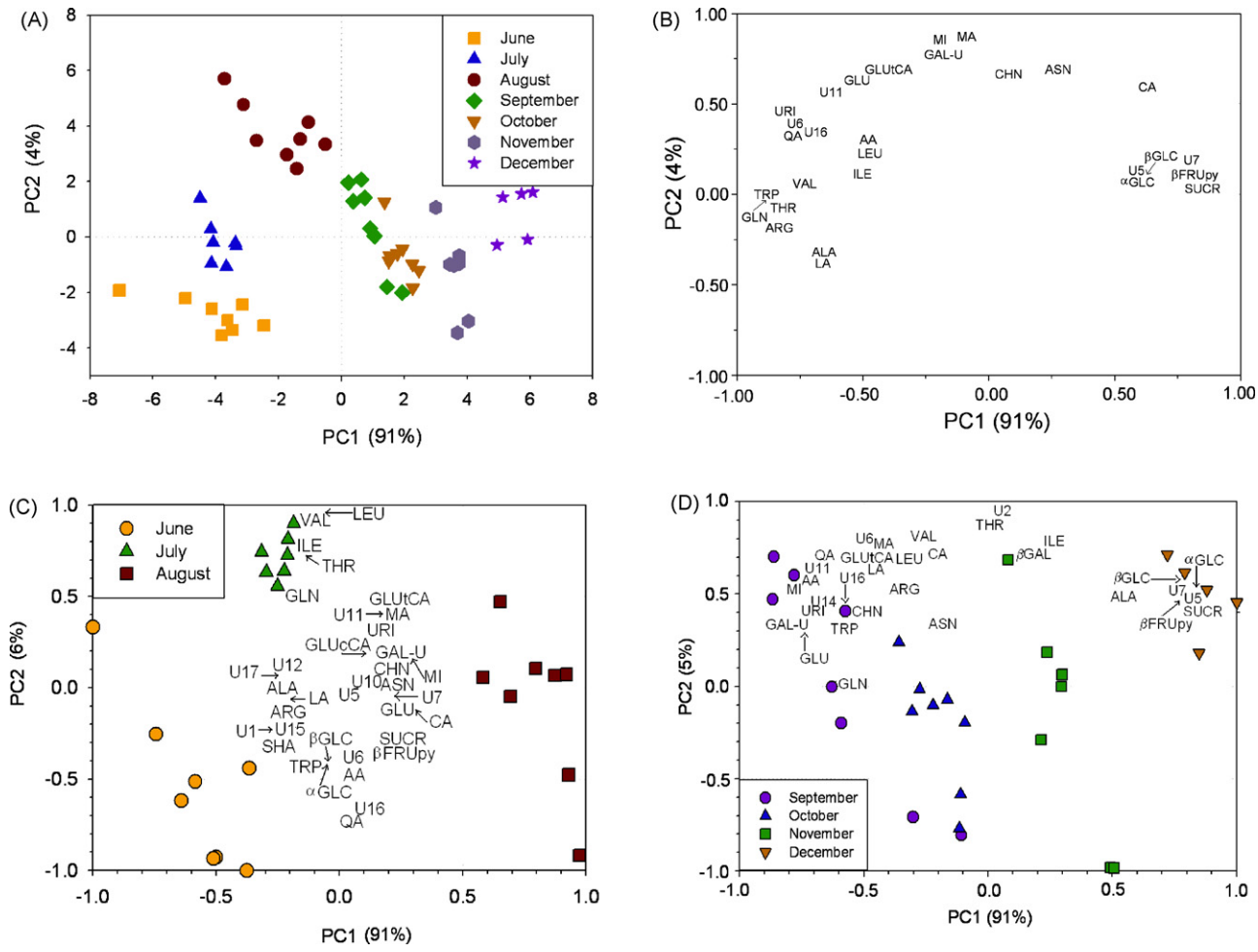

Fig. 5. (A and B) PLS analysis applied to the intensity of 29 ^{1}H resonances always present during the investigated period: (A) plot of PC samples score and (B) plot of variables loadings. (C and D) PLS analyses, reported as biplots, applied to data collected in June, July and August (C), to data collected in September, October, November and December (D). Arrows in (C) and (D) indicate the exact position of the specific variable loading.

kiwifruit growth. The contribution of the variables to this classification is given by the variable loadings reported in Fig. 5B. Many amino acids (VAL, ILE, THR, TRP, LEU, ALA, ARG, GLN), organic acid (LA, AA, QA), URI, and U6, U16 unassigned compounds, present in the highest concentration in the first periods and U5, U7, βFRUpy, SUCR, αGLC, βGLC and CA present in the highest concentration in the last months, mostly contribute to PC1 and are responsible for the grouping according to the harvesting period. On the other hand, MI, GAL-U, MA, CHN, ASN, GLUtCA, GLU, U11 are the variables with the highest contribution to PC2 and are mostly related to the separation of samples harvested in August from the other ones. These findings seem to suggest that August is a "key" month for the kiwifruit development, when a drastic change in the metabolic trend occurs.

In order to investigate in more detail the growth and the ripening processes we decided to perform two different PLS analyses, the first one applied to the data collected in June, July and August, the second one to the data collected in September, October, November and December. In this way, it was possible to take into account also the metabolites present only in the first or in the last harvesting period. Accordingly, in the first PLS analysis the intensity of signals due to SHA, U1, U10, U12, U15, U17, GLUcCA, found only in the first harvesting months, was also taken into account along with the intensity of other 29 metabolites always present. In the second PLS analysis the intensity of signals of U2, U14 and βGAL found only in the last harvesting months, was also taken into account along with the intensity of the other metabolites. The results are reported as biplots in Fig. 5C and D, respectively. In the first PLS, see Fig. 5C, the first two PCs account for the 97% of the variability within the data, PC1 providing for the 91% and PC2 for the 6%. In the second, PCA, see Fig. 5D, the first two PCs account for the 96% of the variability within the data, PC1 providing for the 91% and PC2 for the 5%.

An extremely clear grouping of the data according to the harvesting period was found for the data collected in June, July and August, see Fig. 5C. Samples harvested in July are extremely well grouped being characterized by the highest concentration of some amino acids (LEU, VAL, ILE, THR, GLN). Again, in both PLS analyses, the centroid of each campaign group moves toward high PC1 values according to the kiwifruit growth.

PLS analysis over the early stage (June, July and August) allows a better definition of the processes occurring during the fruit growth: in fact, while PC1 fully confirms the findings from the previous analysis on the whole time range, PC2 also involves variables that are present only in the early period and allows to evaluate changes occurring, for instance, in the shikimic acid pathway. In this respect, some of the metabolites that have been added in the PLS are intermediates of processes that can be observed only in this period: shikimic acid levels are detectable only in June and July indicating its increased utilization over this time range in the production of some metabolites involved in the phenylpropanoids pathway, such as GLUtCA. The observed increase in the GLUtCA level occurring in July and August might be associated to the decrease in trypto-

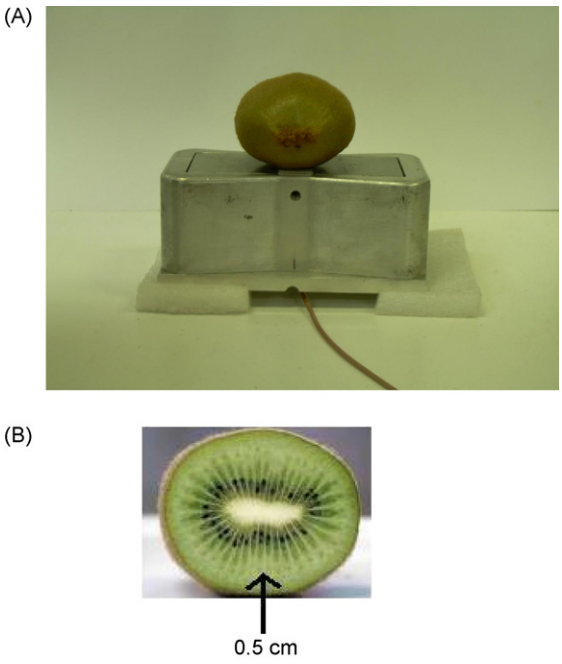

Fig. 6. (A) Measurement of intact kiwifruit with a portable unilateral NMR instrument. (B) Section of kiwifruit showing the depth of measurement with a portable NMR instrument.

phane level. These results suggest an increase of the flux through the phenylpropanoids pathway during the kiwifruit growth only over the early period.

The monitoring of the metabolic profiling of kiwifruits along the season allows information on the chemical composition of the fruit to be obtained. This information may be useful for the industries which use kiwifruit nutrients in the food production.

3.1.6. *Kiwifruit growth using portable unilateral NMR instrument*

The kiwifruits water status was monitored between June and December using an unilateral NMR instrument which allows measurements directly on the entire fruit, without cutting the fruit, see Fig. 6A. Portable NMR instrument allows to obtain information on the relaxation properties of the kiwifruit texture. T_1 and T_2 relaxation times were measured at a depth of about 0.5 cm from the peel surface, see Fig. 6B. As well known, the bulk water gives rise to a mono-exponential decay of the magnetization characterized by a single time constant (T_1 or T_2), whereas water compartmentalized in heterogeneous systems, such as foodstuffs, gives rise to multi-exponential decays characterized by multiple time constants (T_{1i} or T_{2i}, $i = 1, \ldots, n$) [52,53]. Nevertheless, the mixing of water from different sources makes the assignment of relaxation times to particular compartments a difficult task. The extent of averaging depends on the rates of exchange between different intercellular sources, on the intrinsic relaxation times and on cell morphology [53]. The effect of the exchange of water molecules usually affects T_1 more than T_2. As an example, differences in T_1 are rather small and are often not sufficient to identify water sources inside leaf mesophyll. Differences in T_2 are more pronounced, as water exchange over membranes only results in a partial averaging, which depends on the size of the compartments and on the membrane water permeability [54]. As a consequence, in foodstuff, T_2 measurements usually yield more detailed information on the partitioning of water than T_1 measurements [53].

It is important to note that the magnetic field generated by the portable NMR instrument is rather inhomogeneous. Consequently, the inhomogeneous field is a further source of relaxation which shortens the measured T_2 values making them definitively shorter than T_2 values previously reported for kiwifruits [55]. However, we were interested in comparing T_2 trends at different stages of ripening and not in the knowledge of the absolute T_2 values.

In each campaign of measurement nine kiwifruits were monitored measuring T_2 spin–spin relaxation times. As an example, the CPMG decays measured on nine kiwifruits during the campaign of August and December, are reported in Fig. 7A and C respectively. It is easy to observe that the decays measured in December, Fig. 7C, are all much longer than those measured in August, Fig. 7A, suggesting that the CPMG decays lengthen according to the kiwifruit stage of ripening. It must be pointed out that the spread of the decays observed in Fig. 7A and C respectively, reflects small differences in the state of ripening among the investigated kiwifruits. To better visualize these results, the CPMG decays were inverted to obtain the corresponding T_2 distributions, see Fig. 7B and D. In this representation, the maxima (peaks) of the distribution are centred at the corresponding most probable T_2 values, while peaks areas correspond to the relative amount of the T_2 components. In Fig. 7B a typical distribution measured in August is reported with a peak centred at a T_2 value of about 4 ms and another peak centred at a T_2 value of about 11 ms. Whereas in December, see Fig. 7D, the two components lengthen to about 8 and 21 ms, respectively.

In order to obtain a trend of T_2 as a function of the monitoring period, the average $\bar{T}_{2a}$ and $\bar{T}_{2b}$ values, measured on nine kiwifruits during each campaign of measurements, were reported along with the standard deviation, see Fig. 7E and F, respectively. The short $\bar{T}_{2a}$ component shows a rather constant value of about 4 ms until October, then, a clear increment up to 8 ms is observed until December. The long $\bar{T}_{2b}$ component shows a rather constant value of about 14 ms until September, followed by a net increment until December up to 18 ms.

Because we were also interested to know whether T_2 might be also a suitable parameter to monitor the effect of the storage, a further campaign of measurement was performed in February on kiwifruits harvested in December and stored at 4 °C for two months. $\bar{T}_{2a}$ and $\bar{T}_{2b}$ values measured in February were also reported in Fig. 7E and F and were found to be longer than values measured in December. According to this result we may safely assess that T_2 lengthens during the storage period at low temperature. As a consequence, T_2 seems to be a suitable parameter to monitor the ripening as well as the time of storage of kiwifruits.

The water status of Hayward kiwifruits has been previously investigated using quantitative Magnetic Resonance Imaging [56]. MRI has shown distinct differences between the relaxation properties of flesh, locule and cores tissue at a particular sampling date as well as during the season but no consistent association has been found between relaxation parameters and metabolic content. In agreement with the conclusions reported in the case of quantitative MRI, our results also show that the relaxation parameters measured with the portable NMR instrument show a temporal trend with the season of monitoring. The interpretation of this trend is not easy since it cannot be performed only on the basis of changes in metabolic composition but requires a detailed, intimate knowledge of the system. This trend cannot be related, in a simple way, to changes in the metabolic composition, which describe only one aspect, although significant, of the complex phenomenon of fruit development. For instance the increase of soluble mono- and disaccharides during the fruit development is consistent with the progressive disappearance of starch and with the presence of different enzymatic processes which can also contribute to the fruit texture changes.

However, as previously observed [24], the tendency toward longer relaxation times later in the season is consistent with a changing in the cell structure occurring during the ripening process.

Finally, it is worth to note that, properly optimizing the analytical protocol of measurements, the monitoring of the stage of

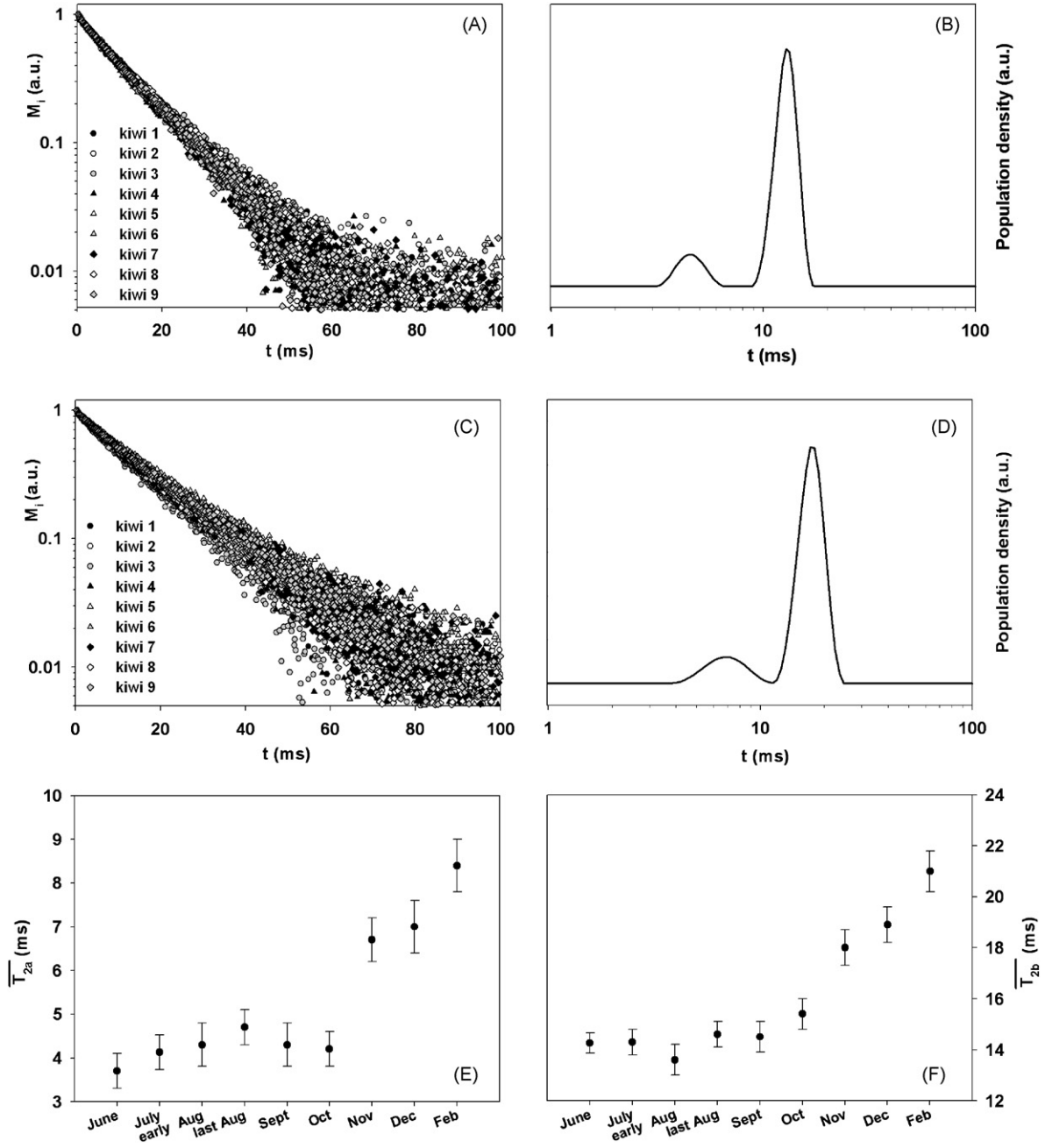

Fig. 7. Decay of the magnetization M_i after applying the CPMG pulse sequence, measured on nine kiwifruits in August (A) and in December (C) (a.u. = arbitrary units). As an example, a T_2 distribution measured in August (B) and one measured in December (D) are reported: the maxima of the distributions are centered at the corresponding most probable T_2 values, whereas peak areas correspond to the relative population of the two T_2 components, namely T_{2a} and T_{2b}. Average T_2 values, $\bar{T}_{2a}$ (E) and $\bar{T}_{2b}$ (F) measured on nine kiwifruits vs. the harvesting month, the error bars represent the maximum error calculated with the error propagation theory.

kiwifruits ripening by portable NMR may also be performed directly in field on the fruit attached to the tree [27].

References

[1] T.W.M. Fan, Prog. Nucl. Magn. Reson. Spectrosc. 28 (1996) 161–219.
[2] L. Mannina, M. Cristinzio, A.P. Sobolev, P. Ragni, A.L. Segre, J. Agric. Food Chem. 52 (2004) 7988–7996.
[3] L. Mannina, A.P. Sobolev, D. Capitani, N. Iaffaldano, M.P. Rosato, P. Ragni, A. Reale, E. Sorrentino, I. D'Amico, R. Coppola, Talanta 77 (2008) 433–444.
[4] L. Mannina, A.L. Segre, Grasas y Aceites 53 (2002) 22–33.
[5] A.P. Sobolev, A.L. Segre, R. Lamanna, Magn. Reson. Chem. 41 (2003) 237–245.
[6] A.P. Sobolev, E. Brosio, R. Gianferri, A.L. Segre, Magn. Reson. Chem. 43 (2005) 625–638.
[7] A.M. Gil, I.F. Duarte, I. Delgadillo, I.J. Colquhoun, F. Casuscelli, E. Humpfer, M. Spraul, J. Agric. Food Chem. 48 (2000) 1524–1536.
[8] L. Mannina, F. Marini, M. Gobbino, A.P. Sobolev, D. Capitani, Talanta 80 (2010) 2141–2148.
[9] M. Defernez, Y.M. Gunning, A.J. Parr, L.V.T. Shepherd, H.V. Davies, I.J. Colquhoun, J. Agric. Food Chem. 52 (2004) 6075–6085.
[10] A.K. Mattoo, A.P. Sobolev, A. Neelam, R.K. Goyal, A.K. Handa, A.L. Segre, Plant Physiol. 142 (2006) 1759–1770.
[11] A. Neelam, T. Cassol, R.A. Mehta, A.A. Abdul-Baki, A.P. Sobolev, R.K. Goyal, J. Abbott, A.L. Segre, A.K. Handa, A.K. Matto, J. Exp. Bot. 59 (2008) 2337–2346.
[12] A.P. Sobolev, A.L. Segre, D. Giannino, D. Mariotti, C. Nicolodi, E. Brosio, M.E. Amato, J. Agric. Food Chem. 55 (2007) 10827–10831.
[13] A.P. Sobolev, D. Capitani, D. Giannino, C. Nicolodi, G. Testone, F. Santoro, G. Frugis, M.A. Iannelli, A.K. Mattoo, E. Brosio, R. Gianferri, I. D'Amico, L. Mannina, Nutrients 2 (2010) 1–15.

[14] A.P. Sobolev, G. Testone, F. Santoro, C. Nicolodi, M.A. Iannelli, M.E. Amato, A. Iannello, E. Brosio, D. Giannino, L. Mannina, J. Agric. Food Chem. 58 (2010) 6928–6936.
[15] L. Mannina, M. D' Imperio, D. Capitani, S. Rezzi, C. Guillou, T. Mavromoustakos, M.D. Molero Vilchez, A.H. Fernández, F. Thomas, R. Aparicio, J. Agric. Food Chem. 57 (2009) 11550–11556.
[16] M.A. Martin-Cabrejas, R.M. Esteban, F.J. Lopez-Andreu, K. Waldron, R.R. Selvendran, J. Agric. Food Chem. 43 (1995) 662–666.
[17] E.A. Macrae, J.H. Bowen, M.G.H. Stec, J. Sci. Food Agric. 47 (1989) 401–416.
[18] H. van Gorsel, C. Li, E.L. Kerbel, M. Smits, A.A. Kader, J. Agric. Food Chem. 40 (1992) 784–789.
[19] H.M. Dawes, J.B. Keene, J. Agric. Food Chem. 47 (1999) 2398–2403.
[20] D. Castaldo, A. Lo Voi, A. Trifiro, S. Gherardi, J. Agric. Food Chem. 40 (1992) 594–598.
[21] G. del Campo, I. Berregi, R. Caracena, J.I. Santos, Anal. Chim. Acta 556 (2006) 462–468.
[22] B.P. Hills, Applications of Low Field NMR to Food Science in Annual Reports on NMR Spectroscopy, vol. 58, Academic Press, The Boulevard Langford Lane, Kidlington, Oxford, UK, 2006, pp. 178–227.
[23] R. Gianferri, V. D'Aiuto, M. Delfini, E. Brosio, Food Chem. 102 (2007) 720–726.
[24] A. Raffo, A.R. Gianferri, R. Barbieri, E. Brosio, Food Chem. 89 (2005) 149–158.
[25] R.J.S. Brown, F. Capozzi, C. Cavani, M.A. Cremonini, M. Petracci, G. Placucci, J. Magn. Reson. 147 (2000) 89–94.
[26] H. Raich, P. Blümer, Conc. Magn. Reson. B: Magn. Reson. Eng. 23B (2004) 16–25.
[27] H. Van As, J.E.A. Reinders, P.A. de Jager, P.A.C.M. van der Sanden, T.J. Schaafsma, J. Exp. Bot. 45 (1994) 61–67.
[28] D. Capitani, F. Brilli, L. Mannina, N. Proietti, F. Loreto, Plant Physiol. 149 (2009) 1638–1647.
[29] B. Blümich, J. Perlo, F. Casanova, Prog. Nucl. Magn. Reson. Spectrosc. 52 (2008) 197–269.
[30] B. Blümich, S. Anferova, K. Kremer, S. Sharma, A.L. Segre, Spectroscopy 18 (2003) 18–32.
[31] A. Miccheli, T. Aureli, M. Delfini, M.E. Di Cocco, P. Viola, R. Gobetto, F. Conti, Cell. Mol. Biol. 34 (1998) 591–603.
[32] E.G. Bligh, W.J. Dyer, Can. J. Biochem. Physiol. 37 (1959) 911–917.
[33] S. Braun, H.O. Kalinowski, S. Berger, 150 and More Basic NMR Experiments, second edition, Wiley-VCH, Weinheim, Germany, 1998.
[34] P. Stilbs, Prog. Nucl. Magn. Reson. Spectrosc. 19 (1987) 1–45.
[35] K.F. Morris, P. Stilbs, C.S. Johnson, Anal. Chem. 66 (1994) 211–215.
[36] C.S. Johnson Jr., Prog. Nucl. Magn. Reson. Spectrosc. 34 (1999) 203–256.
[37] K.F. Morris, C.S. Johnson Jr., J. Am. Chem. Soc. 114 (1992) 3139–3141.
[38] L. Eriksson, E. Johansson, N. Kettaneh-Wold, J. Trygg, C. Wikstrom, S. Wold, Multivariate and megavariate data analysis basic principles and applications (Part I), Umetrics AB, Umeå, 2006.
[39] H. Martens, M. Martens, Food Qual. Prefer. 11 (2000) 5–16.
[40] H. Martens, M. Hoy, F. Westad, B. Folkenberg, M. Martens, Chemometr. Intell. Lab. Syst. 58 (2001) 151–170.
[41] G. Eidmann, R. Savelsberg, P. Blümer, B. Blümich, J. Magn. Reson. A 122 (1996) 104–109.
[42] B. Blümich, S. Anferova, S. Sharma, A.L. Segre, C. Federici, J. Magn. Reson. 161 (2003) 204–209.
[43] E. Fukushima, S.B.W. Roeder, Experimental Pulse NMR: A Nuts and Bolts Approach, Addison-Wesley Publishing, Boston, 1981.
[44] H.Y. Carr, E.M. Purcell, Phys. Rev. 94 (1954) 630–638.
[45] S. Meiboom, D. Gill, Rev. Sci. Instrum. 29 (1958) 688–691.
[46] W.H. Press, W.T. Teukolsky, B.P. Vetterling, B.P. Flannery, Numerical Recipes in Chemistry, Cambridge University press, Cambridge, UK, 1994.
[47] E.A. MacRae, J.H. Bowen, M.G.H. Stec, J. Sci. Food. Agric. 47 (1989) 401–416.
[48] R. Schröder, R.P. Nicolas, S.J.F. Vincent, M. Fischer, S. Reymond, R.J. Redgwell, Carbohydr. Res. 331 (2001) 291–306.
[49] I. Nishiyama, T. Fukuda, A. Shimohashi, T. Oota, Food Sci. Technol. Res. 14 (2008) 67–73.
[50] R.L. Bieleski, C.J. Clark, K.U. Klages, Phytochemistry 46 (1997) 51–55.
[51] H. Meyermans, K. Morreel, C. Lapierre, B. Pollet, A. De Bruyn, R. Busson, P. Herdewijn, B. Devreese, J. Van Beeumen, J.M. Marita, J. Ralph, C. Chen, B. Burggraeve, M. Van Montagu, E. Messens, W. Boerjana, J. Biol. Chem. 275 (2000) 36899–36909.
[52] C. Colire, E. Le Rumeur, J. Gallier, J. de Certaines, F. Larher, Plant Physiol. Biochem. 26 (1998) 767–776.
[53] J.E.M. Snaar, H. Van As, Biophys. J. 63 (1992) 1654–1658.
[54] H. van As, J. Exp. Bot. 58 (2007) 743–756.
[55] A. Taglienti, R. Massantini, R. Rotondi, F. Mencarelli, M. Valentini, Food Chem. 114 (2009) 1583–1589.
[56] C.J. Clark, L.N. Drummond, J.S. MacFall, J. Sci. Food Agric. 78 (1998) 349–358.